Graphical Models 76 (2014) 340–354

Contents lists available at ScienceDirect

Graphical Models

journal homepage: www.elsevier.com/locate/gmod

Improved, feature-centric EMD for 3D surface modeling and processing

Jianping Hu [a,b,*], Xiaochao Wang [c], Hong Qin [d]

[a] College of Sciences, Northeast Dianli University, Jilin 132012, China
[b] Key Laboratory of Symbolic Computation and Knowledge Engineering of Ministry of Education, Jilin University, Changchun 130012, China
[c] State Key Laboratory of Virtual Reality Technology and Systems, Beihang University, Beijing 100191, China
[d] Department of Computer Science, Stony Brook University (SUNY), Stony Brook, NY 11794-4400, USA

ARTICLE INFO

Article history:
Received 1 March 2014
Accepted 17 March 2014
Available online 3 April 2014

Keywords:
Feature-centric EMD
Measure of mean curvature
Filter design
Detail transfer
Feature-preserving smoothing

ABSTRACT

Since late 1990s, Empirical Mode Decomposition (EMD) starts to emerge as a powerful tool for processing non-linear and non-stationary signals. Nonetheless, the research on exploring EMD-relevant techniques in the domain of geometric modeling and processing is extremely rare. Directly applying EMD to coordinate functions of 3D shape geometry will not take advantage of the attractive EMD properties. To ameliorate, in this paper we articulate a novel 3D surface modeling and processing framework founded upon improved, feature-centric EMD, with a goal of realizing the full potential of EMD. Our strategy starts with a measure of mean curvature as a surface signal for EMD. Our newly-formulated measure of mean curvature is computed via the inner product of Laplacian vector and vertex normal. Such measure is both rotation-invariant and translation-invariant, facilitates the computation of different scale features for original surfaces, and avoids boundary shrinkage when processing open surfaces. Moreover, we modify the original EMD formulation by devising a feature-preserving multiscale decomposition algorithm for surface analysis and synthesis. The key idea is to explicitly formulate details as oscillation between local minima and maxima. Within our novel framework, we could accommodate many modeling and processing operations, such as filter design, detail transfer, and feature-preserving smoothing and denoising. Comprehensive experiments and quantitative evaluations/comparisons on popular models have demonstrated that our new surface processing methodology and algorithm based on the improved, feature-centric EMD are of great value in digital geometry processing, analysis, and synthesis.

1. Introduction

In 1998, Empirical Mode Decomposition (EMD) was developed for processing 1D non-linear and non-stationary signals by Huang et al. [9]. The central idea is to decompose a signal into a finite number of intrinsic mode functions (IMFs) with multi-scale oscillatory modes and a residue with monotonic trend, where the first IMF starts with the finest, temporal/spatial scale, and the subsequent IMFs gradually exhibit coarser, temporal/spatial scales (Fig. 1). The IMFs represent the natural oscillatory modes embedded in signals and can play a role of the basis functions. Such basis functions can be computed by operating on the local extremum sequence, while extracting the local energy associated with the intrinsic temporal/spatial scales of the signal itself. Consequently, such decomposi-

* Corresponding author at: College of Sciences, Northeast Dianli University, Jilin 132012, China.
E-mail address: hjp307@gmail.com (J. Hu).

http://dx.doi.org/10.1016/j.gmod.2014.03.006
1524-0703/

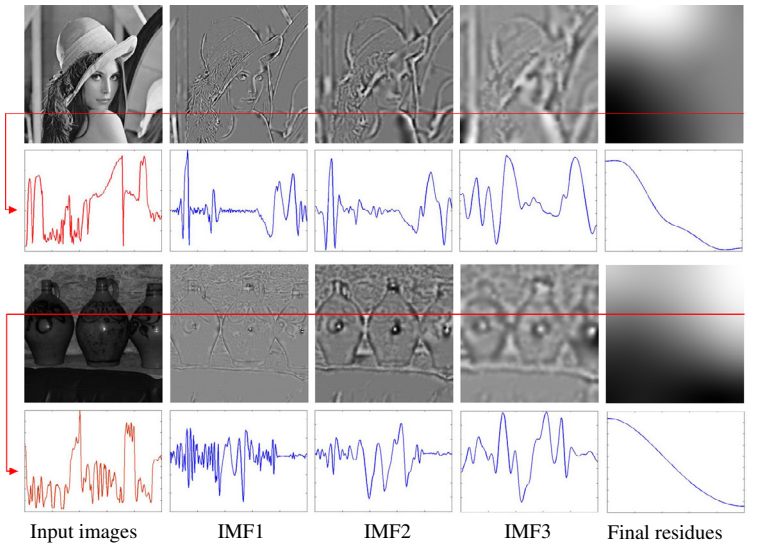

Fig. 1. EMD for lena and vase images using the method of Wang et al. [34], where the images are treated as functions defined over a planar domain. All IMF images are scaled into [0,255] for better visualization.

tion is fully data-driven and different from the other multiscale analysis technologies (e.g., Fourier analysis, short-time Fourier analysis, and wavelet analysis), which (in contrast) characterize the scale of a signal using predefined basis functions.

Ever since its inception, EMD has been considered as a revolutionary method in signal analysis and processing due to its above-documented special properties, and has given rise to a wide variety of applications in 1D and 2D data analysis and processing [10], such as biomedical engineering [24], speech processing [8], image fusion [38], image compression [12], image analysis [19], etc. However, there is little literature on how to apply EMD to 3D surface processing [22,34]. Qin et al. [22] first converted coordinate functions of 3D surfaces to 2D planar signals with the help of spherical parameterization, and then computed EMD representations using the conventional 2D EMD method, where global mesh parameterization is a pre-requisite (which might limit its application scopes). To overcome this limitation, Wang et al. [34] generalized 1D EMD to surfaces directly without resorting to any surface parameterization technique. Their method generates the upper and lower envelopes of a function defined on a 3D surface by computing a biharmonic field with Dirichlet boundary conditions. This generalized EMD on surfaces could be directly applied to coordinate functions of 3D geometry for surface filtering.

The primary reasons about the scarce use of EMD in 3D surface processing are twofold. First, 3D surfaces are represented by 3 coordinate functions independent of each other, yet meaningful geometry features must be characterized by simultaneously utilizing multiple coordinates in the computation of differential properties. However, the naive integration of 3 independent decompositions could not properly lead to surface features of different scales, therefore losing the inherent advantage of EMD completely. In the mean time, undesirable effects inherited from 1D EMD near boundary will be enlarged if simply combining separate decompositions of 3 coordinate functions, i.e., boundary shrinkage will emerge when applying EMD to open surfaces, and this becomes unacceptable in 3D surface processing. Second, the feature awareness of 3D surfaces (e.g., sharp edges and corners) is critical in many tasks of 3D surface processing, such as surface denoising and editing. However, the original EMD is only designed to obtain IMFs at different scales from the given data and does not have the feature-aware property. Hence, it could not preserve features during processing.

In this paper, we make significant efforts to tackle the aforementioned problems, with an ambitious goal of adapting EMD to 3D surface processing. We articulate a novel 3D surface modeling and processing framework founded upon a new, improved, feature-centric EMD. We first employ a measure of mean curvature as the input signal of EMD, which can be computed by the inner product of Laplacian vector at each vertex and its corresponding normal. It can help get different scale features of the original surface and prevent the boundary shrinkage when computing EMD for open surfaces. Furthermore, we design a new EMD formulation on 3D surfaces by devising a feature-preserving multiscale decomposition algorithm for surface analysis and synthesis, which defines detail as oscillation between local minima and maxima. This is motivated by the edge-preserving multiscale image decomposition based on extremal envelopes [29]. As a result, within our novel framework, we could accommodate many modeling and processing operations, such as filter design, detail transfer, feature-preserving smoothing and denoising. Fig. 2 illustrates the pipeline of our framework.

Our major contributions in this paper are summarized as follows:

1. We develop a novel 3D surface analysis and processing framework where EMD takes on the center stage. We make use of a measure of mean curvature as an input

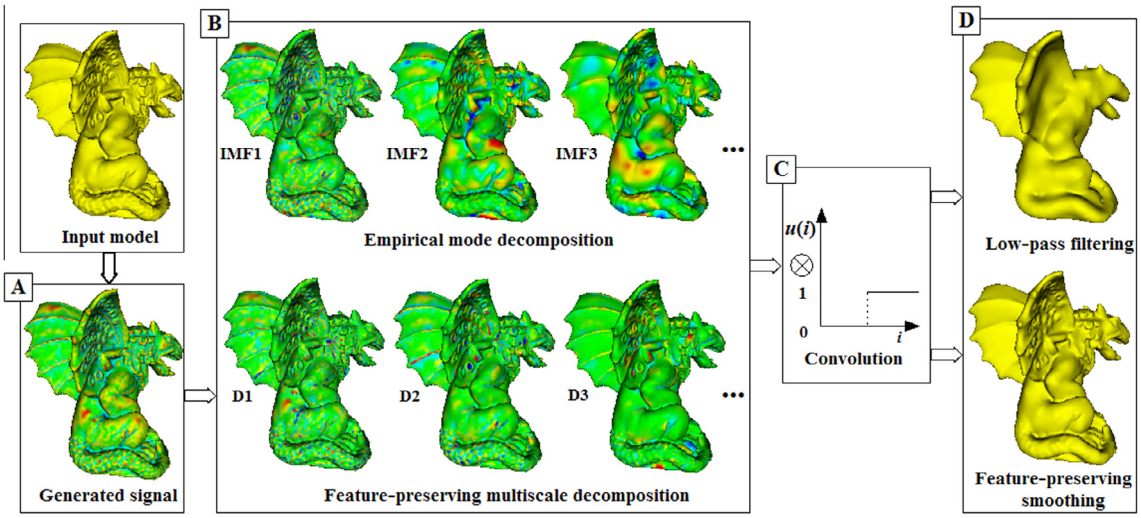

Fig. 2. The pipline of our framework based on the improved, feature-centric EMD for 3D surface modeling and processing. (A) Compute the signal about the measure of mean curvature of the input model. (B) Decompose the signal by EMD or feature-preserving multiscale decomposition. (C) Process the IMFs and the detail levels. (D) Reconstruct surfaces from the modified signal in the least-squares sense.

signal of EMD. This can help extract different scale features of the original surface, and prevent the boundary shrinkage when handling open surfaces.

2. We modify the original EMD formulation on 3D surfaces by designing a feature-preserving multiscale decomposition algorithm for surface analysis and synthesis, which overcomes the limitation of the original EMD on 3D surfaces. The newly-devised EMD formulation now becomes feature-aware and enables feature-preserving operations.
3. Our framework could facilitate many modeling and processing operations, such as filter design, detail transfer, and feature-preserving smoothing and denoising, which are both effectively and powerful, and collectively demonstrate more potential of EMD in 3D surface modeling and processing.

2. Related work

We shall briefly review related works in Empirical Mode Decomposition (EMD), 3D surface processing based on time–frequency analysis, and feature-preserving surface smoothing.

2.1. Empirical mode decomposition

EMD was first introduced by Huang et al. [9] and is a fully adaptive multiscale decomposition method. It generates IMFs by a sifting process, which needs to find local extrema points (maxima and minima) and subsequent interpolation of those points in each iteration of the process by cubic splines to generate upper and lower envelopes [9]. The time frequency distribution of the signal from each IMF can be generated by Hilbert transform. This method can overcome the limitation of Fourier analysis, short-time Fourier analysis and wavelet analysis that essentially depend on the methods for processing linear and stationary signals, and has been applied to various data analysis and processing fields [8,10,12,19,24,38].

This decomposition technique has also been extended to high dimensional signals (e.g., 2D and 3D signals [12,15,19,23,38]). As for signals on 3D surfaces, Qin et al. [22] first transformed coordinate functions of 3D surfaces to 2D planar signals with the help of spherical parameterization, and then obtained the EMD representations by the exiting 2D EMD methods. Unfortunately, it is utmost difficult to generalize such method to process models with high genus and complicated structure due to the use of global mesh parameterization. To overcome this limitation, Wang et al. [34] directly generalized 1D EMD to 3D surfaces, which generates the upper and lower envelopes of a function by computing a biharmonic field with Dirichlet boundary conditions.

The classical 1D EMD does not have the feature-preserving property, and its direct generalization to 2D or 3D surfaces will not have such property either. An edge-preserving multiscale image decomposition was proposed by Suber et al. [29], which is inspired by EMD and treats details as oscillation between local minima and maxima. Motivated by their method, we improve the original EMD formulation on 3D surfaces by devising a new feature-preserving multiscale decomposition algorithm for surface analysis and synthesis. However, the feature-preserving multiscale decomposition on surfaces is much more technically challenging than that of 2D images because sharp edges and corners of 3D geometry will be blurred when we attempt to use currently available methods to extract details by subtracting the average of extremal envelopes interpolated from local extrema.

2.2. 3D Surface processing based on time–frequency analysis

Classical time–frequency analysis tools for signal processing, such as Fourier analysis, short-time Fourier

analysis, and wavelet analysis, can transform a signal to a sum of different frequency components, which are oftentimes very helpful for signal processing and have been generalized to 3D surfaces.

Taubin [30] attempted to design and analyze approximations of low-pass filters using the similarity between the eigenvectors of the graph Laplacian and the basis functions used in the discrete Fourier transform. Instead of using Fourier analysis as a theoretical tool to analyze approximations of filters, Vallet and Levy computed the Fourier transform of the signal on the mesh directly [32]. Spherical harmonic analysis, which is also called Fourier analysis on the unit sphere, was employed to conduct surface filtering, surface reconstruction, and texture transfer [17,41]. The short-time Fourier transforms are also used for signal processing of point cloud surfaces, where each surface patch is resampled on a regular grid using a fast scattered data approximation [20].

Compared to Fourier analysis, wavelet analysis has locality in both time/space and frequency domain, and is a more powerful tool for signal processing. Various kinds of wavelets have been proposed for 3D surface processing, such as subdivision wavelets [6,14], spherical wavelets [25] and diffusion wavelets [3,7]. Most of the above-mentioned wavelets require certain preprocessing operations, for example, subdivision wavelets require that the surfaces must be the multiscale meshes generated by simplification and subdivision, spherical wavelets need that the surface must be parameterized over a sphere. In contrast, diffusion wavelets do not need subdivision, leading to more flexibility in practical use.

As a novel fully adaptive and data-driven time–frequency analysis method, EMD has been also used for 3D surface processing. The existing methods directly apply EMD to coordinate functions to conduct 3D surface filtering [22,34], which cannot take advantage of the attractive EMD properties and can cause boundary shrinkage when processing open surfaces due to the end effects inheriting from 1D EMD along surface boundaries. In this paper, we develop a novel framework based on EMD using a measure of mean curvature as an input signal of EMD, and our motivation is to broaden the application scopes and utilities of EMD. Specifically, our goal is to obtain features of different scales by decomposing the original surface and overcome the shortcoming of boundary shrinkage when handling open surfaces.

2.3. Feature-preserving surface smoothing

Although surface smoothing can be naively achieved by a low-pass filter, much more work must be introduced in order to preserve features such as sharp edges and corners in 3D surfaces during smoothing and denoising processes.

Laplacian smoothing is the most commonly-used surface smoothing techniques. Unfortunately, it is not feature-preserving. To over this limitation, Nealen et al. [18] and Liu et al. [13] proposed similar Laplacian smoothing schemes by setting the vertex Laplacians to zero and reconstructing the surface with geometric feature constraints.

Some feature-preserving surface smoothing techniques are based on anisotropic diffusion which generalizes feature-preserving anisotropic diffusion in image processing to anisotropic geometric diffusion on surfaces [1,2,36]. Such approaches try to preserve the geometric features by introducing anisotropic heat diffusion, which are mainly dictated by the heat diffusion equation over surfaces. In principle, the expensive computation of energy gradients and Hessians or eigen-decomposition is unavoidable.

Some other feature-preserving surface smoothing techniques [4,33,35,39,40] are based on bilateral filter from image processing, which was first extended to surfaces by Fleishman et al. [4]. The bilateral filter had also been used for smoothing the Laplacian coordinates and face normals and preserving features [33,40]. However, it is difficult to determine the best parameters of spatial locations and signals, additional processes must be introduced for better feature-preserving [35].

Unlike the aforementioned methods, Wang et al. [34] proposed an approach based on extremal envelopes to conduct multiscale surface decomposition with the property of feature-preserving motivated by an edge-preserving multiscale image decomposition [29], which cannot preserve feature well and is only limited to watertight surfaces. In our current work, we use our feature-preserving multiscale decomposition algorithm instead of the conventional EMD to serve as a solid theoretical foundation for our novel surface processing framework with which we not only can preserve sharp features well but can handle open surfaces as well.

3. Measure of mean curvature and surface signals

Laplace operator is a second-order differential operator and can be extended to 3D surfaces, called Laplace–Beltrami operator (manifold Laplacian). It can measure the local deviation from the smooth thin-plate surface and record information about the local shape. The discrete Laplace operator has been used in various tasks of geometric processing, for example, mesh smoothing, mesh editing, and shape interpolation [26].

Let $M = (\mathbf{V}, \mathbf{K})$ be a triangular mesh which represents a discretization of a 2-manifold in 3D, where $\mathbf{V}$ denotes a set of vertices $\{\mathbf{v}_i = (x_i, y_i, z_i) \in R^3,\ i = 1, \ldots, n\}$, and $\mathbf{K}$ contains all the adjacency information of the mesh including edges and faces. The discrete Laplace operator on a meshed surface can be computed by weighted average over the neighborhood

$$\Delta(\mathbf{v}_i) = \sum_{j \in N(i)} w_{ij}(\mathbf{v}_j - \mathbf{v}_i), \tag{1}$$

where $N(i)$ is the vertex set of the 1-ring neighbors of vertex $\mathbf{v}_i$.

If we employ the cotangent weights,

$$w_{ij} = \cot \alpha_{ij} - \cot \beta_{ij}, \tag{2}$$

the discrete Laplace vector is parallel to the vertex normal and becomes [16]

$$\Delta(\mathbf{v}_i) = 4 \mid \Omega_i \mid \kappa_i \mathbf{n}_i, \tag{3}$$

where α_{ij} and β_{ij} are the angles opposite to the mesh edge (i, j), $\mid \Omega_i \mid$ and κ_i are the Voronoi cell area and the mean curvature at $\mathbf{v}_i$, respectively.

We define a signal using the inner product of discretized Laplacian vector and the corresponding vertex normal as follows:

$$\mathbf{s}(\mathbf{v}_i) = (\Delta(\mathbf{v}_i) \cdot \mathbf{n}_i), \tag{4}$$

which can be regarded as a measure of mean curvature and is the sampling-density-dependent version of mean curvature, i.e., mean curvature times the one-ring area.

Obviously, Eq. (4) is both rotation-invariant and translation-invariant and can be used as a signal serving as the input of EMD while retaining all the attractive EMD properties. Furthermore, it can be effectively used to reconstruct meshes. Such procedure is common in the existing Laplacian surface processing methods [26,27].

Laplacian vector computed with the cotangent weights (Eq. (2)) has a strong tangential component for each boundary vertex of open surfaces since the outer edges are missing and there is no mechanism to compensate the surface tension. Some solutions for this problem are proposed in [31,36]. We use the method of Wang et al. [36] to combat this problem. The process is as follows,

1. Project each boundary vertex $\mathbf{v}_i$ and its one-ring vertices $\mathbf{v}_j,\ j \in N(i)$ onto its normal plane to generate $\mathbf{v}'_i$ and $\mathbf{v}'_j,\ j \in N(i)$.
2. Compute the Laplacian vector in the normal plane as $\Delta(\mathbf{v}_i) = \sum_{j \in N(i)} w_{ij}\left(\mathbf{v}'_j - \mathbf{v}'_i\right)$, where w_{ij} is computed using Eq. (2).

The Laplacian vector computed this way is parallel to the normal of the boundary vertex and can remove tangential component of the original cotangent Laplacian vector.

4. Signal decomposition based on measure of mean curvature

We use two methods to decompose the signal about the measure of mean curvature, one is the classical EMD algorithm to extract IMFs encoded different scale features of surfaces, and another is our improved feature-preserving multiscale decomposition method of EMD to generate a feature-aware decomposition.

4.1. Empirical mode decomposition on 3D surfaces

EMD on 3D surfaces proposed by Wang et al. [34] extends 1D EMD to 3D surfaces. It can adaptively extract a finite number of intrinsic mode functions (IMFs) from the given function defined on a 3D surface by a sifting processing, which represents the intrinsic oscillatory modes imbedded in the data (Fig. 1). Specifically, it can decompose a function $\mathbf{g}$ defined on a 3D surface, i.e., $\mathbf{g} : M \to R$ as

$$\mathbf{g} = \sum_{k=1}^{N} \mathbf{f}_k + \mathbf{r}_N, \tag{5}$$

where $\mathbf{f}_k,\ k = 1, \ldots, N$ are IMFs and $\mathbf{r}_N$ is the corresponding residue (Figs. 1 and 3). They can be computed using Algorithm 1.

Algorithm 1. EMD Algorithm on 3D Surfaces

Input: a function $\mathbf{g}$ defined on a surface M
Initialization: set the initial residue and the initial index of IMFs, $\mathbf{r}_0 = \mathbf{g},\ k = 1$;
1: **repeat**
2: $\mathbf{h}_0 = \mathbf{r}_{k-1},\ j = 1$;
3: **for** each j **do**
4: find all local extrema of $\mathbf{h}_{j-1}$ (Section 4.1.1);
5: interpolate all local maxima (resp. minima) of $\mathbf{h}_{j-1}$ to obtain the upper envelopes and the lower envelopes $\mathbf{Uh}_{j-1}$ and $\mathbf{Dh}_{j-1}$ (Section 4.1.2);
6: compute the local mean $\mathbf{m}_{j-1}$ of $\mathbf{h}_{j-1}$ using $\mathbf{m}_{j-1} = (\mathbf{Uh}_{j-1} + \mathbf{Dh}_{j-1})/2$;
7: $\mathbf{h}_j = \mathbf{h}_{j-1} - \mathbf{m}_{j-1}$;
8: **if** $\mathbf{h}_j$ satisfies the stopping criteria of the sifting process (Section 4.1.3) **then**
9: obtain the k-th IMF $\mathbf{f}_k = \mathbf{h}_j$ and the k-th residue $\mathbf{r}_k = \mathbf{r}_{k-1} - \mathbf{f}_k$;
10: $k = k + 1$;
11: break;
12: **else**
13: $j = j + 1$;
14: **end if**
15: **end for**
16: **until** the residue $\mathbf{r}_k$ is a constant or a monotonic function, or the number of IMFs is more than a given threshold
Output: all IMFs $\mathbf{f}_k,\ k = 1, \ldots, N$ and the residue $\mathbf{r}_N$.

4.1.1. Extremum definition

As for the function $\mathbf{g}$ defined on a 3D surface, if $\mathbf{g}(\mathbf{v}_i)$ satisfies

$$\mathbf{g}(\mathbf{v}_i) \geqslant \mathbf{g}(\mathbf{v}_j), \quad j \in N(i) \text{or} \mathbf{g}(\mathbf{v}_i) \leqslant \mathbf{g}(\mathbf{v}_j), \quad k \in N(i),$$

then $\mathbf{v}_i$ is defined as a local maximum or a local minimum.

4.1.2. Interpolation method for computing envelopes

Biharmonic interpolation is used to generate the upper and lower envelopes in EMD on surfaces [34], which is a natural extension of the cubic spline to 3D surface and minimizes the thin-plate energy of a function Φ defined on a 3D surface M,

$$\int_M (\triangle_M \Phi)^2 \, dV. \tag{6}$$

The corresponding Euler–Lagrange equation of the energy formulation (Eq. (6)) is

$$\triangle_M^2 \Phi = 0, \tag{7}$$

where $\triangle_M$ is the Laplace–Beltrami operator on the surface M.

Specifically, given interpolated anchors and corresponding values $\{(\mathbf{v}_i, \mathbf{g}(\mathbf{v}_i)), i \in C\}$, the interpolation function $\Phi = (\Phi(\mathbf{v}_1), \Phi(\mathbf{v}_2), \ldots, \Phi(\mathbf{v}_n))$ can be computed by solving the following $n \times n$ linear system

$$\mathbf{L}^2 \cdot \Phi = 0, \quad s.t., \ \Phi(\mathbf{v}_i) = \mathbf{g}(\mathbf{v}_i), \quad i \in C, \tag{8}$$

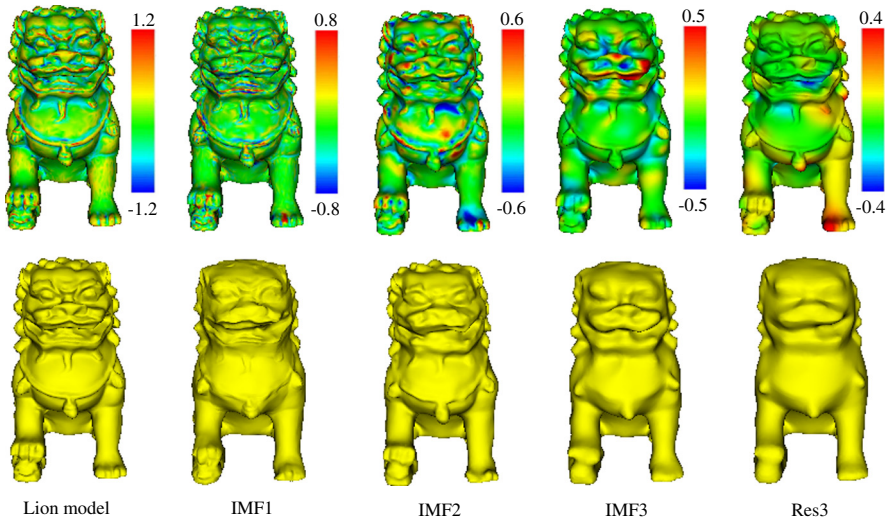

Fig. 3. EMD using the measure of mean curvature of the lion model as an input signal. In order to visualize IMFs, meshes corresponding to IMFs (shown in the second row) are reconstructed using its IMFs and the 3rd residue (shown in the first row) of the input signal, respectively.

where C is the interpolated anchor set for the scalar function $\mathbf{g}$, and $\mathbf{L}$ is the $n \times n$ discretized Laplacian matrix with the following elements

$$\mathbf{L}_{ij} = \begin{cases} \sum_{k \in N(i)} w_{ik}, & j = i \\ -w_{ij}, & j \in N(i) \\ 0, & \text{otherwise} \end{cases} \tag{9}$$

where $w_{ij} = \frac{1}{2A_i}(\cot \alpha_{ij} - \cot \beta_{ij})$ [16], α_{ij} and β_{ij} are the angles opposite to the mesh edge (i,j), and A_i is the Voronoi area of vertex $\mathbf{v}_i$.

The direct elimination method in [5] can be used to solve this biharmonic field with Dirichlet boundary conditions (Eq. (8)), which eliminates from the linear system matrix the variables corresponding to the anchor vertices with known constraints. The unknown interpolation function values can be computed by solving the rearranged linear system using Cholesky factorization.

4.1.3. Stopping criteria of the sifting process

The essence of the stopping criteria of the sifting process is to judge whether the function after being sifted once is an IMF. It is controlled by limiting the size of the standard deviation SD. The sifting process is stopped if SD falls below a threshold. It is computed from the two consecutive sifting results $\mathbf{h}_j$ and $\mathbf{h}_{j-1}$ at all vertices as follows:

$$SD = \sum_{i=1}^{n} \frac{|\mathbf{h}_j(\mathbf{v}_i) - \mathbf{h}_{j-1}(\mathbf{v}_i)|^2}{|\mathbf{h}_{j-1}(\mathbf{v}_i)|^2}. \tag{10}$$

The typical threshold value of the stopping criteria is set between 0.1 and 0.3 just like that in the original 1D EMD. Generally speaking, a smaller value would lead to more IMFs, while a larger value would lead to less IMFs. The default value in this paper is 0.1.

4.2. Feature-preserving multiscale decomposition on 3D surfaces

We modify the original EMD formulation on 3D surfaces by devising a feature-preserving multiscale decomposition algorithm for surface analysis and synthesis to overcome the limitation of the EMD on 3D surfaces. The key idea is to explicitly formulate details as oscillation between local minima and maxima which is similar to the edge-preserving image multiscale decomposition method in spirit [29], but we must do extra work to preserve sharp edges and corners since they will be blurred when extracting details by subtracting the average of extremal envelopes interpolated from local extrema (Fig. 4(c)).

Our feature-preserving multiscale decomposition method uses only one feature-preserving smoothing step to get the detail level instead of one iterative sifting processing step to accelerate the decomposition. The smoothing step treats the mean of the upper and lower envelope interpolating the maxima and minima independently as the smoothing function. The detail level can be extracted by substracting the smoothing function. In order to extract multiscale details, we enlarge the extrema-location kernel with the increasing of the smoothing number k, i.e, k-ring neighborhood of each vertex. In addition, we add the sharp features as constraints extracted before multiscale decomposition to avoid their blurring.

Let $\mathbf{g}$ be a function on a meshed 3D surface M, $\mathbf{g} : M \to R$, our feature-preserving multiscale decomposition algorithm can compute

$$\mathbf{g} = \sum_{k=1}^{N} \mathbf{D}_k + \mathbf{r}_N, \tag{11}$$

where $\mathbf{D}_k$, $k = 1, \ldots, N$ are details of different levels and $\mathbf{r}_N$ is the N-th level residue (Fig. 5). They can be computed using Algorithm 2.

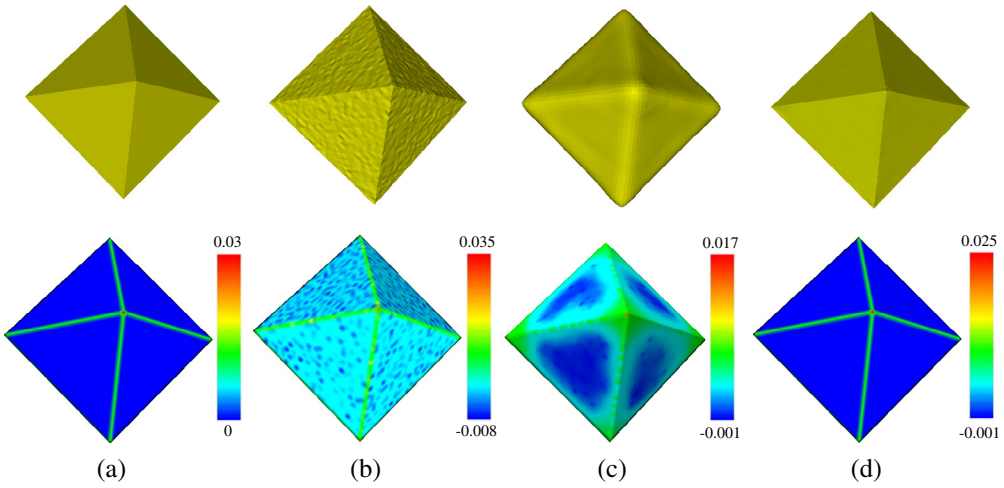

Fig. 4. Illustration of the function of feature constraints in our feature-preserving multiscale decomposition. (a) The octahedral model as a ground truth. (b) The model artificially corrupted by Gaussian noise of 5% of mean edge length. (c and d) are the 3rd residue using our feature-preserving multiscale decomposition without feature constraints and with feature constraints, respectively. The first row contains the mesh models and the second row shows the visualizations of their signals about the measure of mean curvature.

Algorithm 2. Feature-preserving multiscale decomposition algorithm on 3D surfaces

Input: a function $\mathbf{g}$ defined on a meshed surface M and the feature vertex set G
Initialization: set the initial residue and the initial decomposition level, $\mathbf{r}_0 = \mathbf{g},\ k = 1$;
1: **repeat**
2: find all local maxima and minima of $\mathbf{r}_{k-1}$ (Section 4.2.1);
3: interpolate all local maxima (resp. minima) to obtain the upper envelopes $\mathbf{Ur}_{k-1}$ and the lower envelopes $\mathbf{Dr}_{k-1}$ with feature vertex constraint G, and then get the local mean $\mathbf{m}_{k-1}$ using $\mathbf{m}_{k-1} = (\mathbf{Ur}_{k-1} + \mathbf{Dr}_{k-1})/2$ (Section 4.2.2);
4: extract the k-th detail level $\mathbf{D}_k$ using $\mathbf{D}_k = \mathbf{r}_{k-1} - \mathbf{m}_{k-1}$ and the k-th residue using $\mathbf{r}_k = \mathbf{m}_{k-1}$;
5: $k = k + 1$;
6: **until** the number of detail levels is more than a given threshold
Output: all detail levels $\mathbf{D}_k,\ k = 1, \ldots, N$ and the residue $\mathbf{r}_N$.

4.2.1. Feature extraction and extremum definition

4.2.1.1. Feature extraction. Feature extraction has been a well-studied research area in many scientific fields. In this paper, we do not discuss how to extract the features but only use the existing method [37] to detect sharp features (Fig. 6), which combines normal tensor voting with neighbor supporting and is robust to noises.

4.2.1.2. Extremum definition. Different from the extremum definition in EMD on 3D surfaces, we enlarge the extrema-location kernel with the increasing decomposition level and set a parameter to incorporate more vertices as extrema in order to preserve features. Specifically, in the kth decomposition, if $\mathbf{g}(\mathbf{v}_i)$ satisfies the following condition:

$$| N_{\mathbf{g}}^{+}(\mathbf{v}_i) | \geqslant t \, | N_k(i) |,$$

where $N_{\mathbf{g}}^{+}(\mathbf{v}_i) = \{j \mid \mathbf{g}(\mathbf{v}_i) \geqslant \mathbf{g}(\mathbf{v}_j),\ j \in N_k(i)\}$, $|\cdot|$ denotes the element number of a set, $t \in [0, 1]$ is a parameter, and $N_k(i)$ denotes the k-ring neighbors of $\mathbf{v}_i$, then $\mathbf{v}_i$ is defined as a local maximum. The local minimum can be determined in a similar fashion. If t is much smaller, more extrema are involved. The default value of t is 0.8 in this paper, and we will discuss it in more details in Section 6.

It should be pointed out that some feature vertices extracted beforehand may be included into the extremum set. We must remove them from the extremum set to avoid their blurring when extracting details by subtracting the average of extremal envelopes interpolated from local extrema.

4.2.2. Interpolation method for computing envelopes

In EMD on 3D surfaces [34], biharmonic interpolation is used to generated the upper and lower envelopes, which is very similar to the approaches using the uniform discretization of the Laplace operator and soft (instead of hard) constraints [27].

We use the similar idea to compute the interpolation function Φ for the interpolated anchors and corresponding values $\{(\mathbf{v}_i, \mathbf{g}(\mathbf{v}_i)),\ i \in C\}$, but edge-aware weights are used to discretize the Laplace operator, which are widely used during feature-preserving image and surface processing [4,11,29]. Meanwhile, the feature vertex index set $G = \{s_1, s_2, \ldots, s_m\}$ is regarded as soft constraints. Specifically, the interpolation function $\Phi = (\Phi(\mathbf{v}_1), \Phi(\mathbf{v}_2), \ldots, \Phi(\mathbf{v}_n))$ can be generated by minimizing the following energy function:

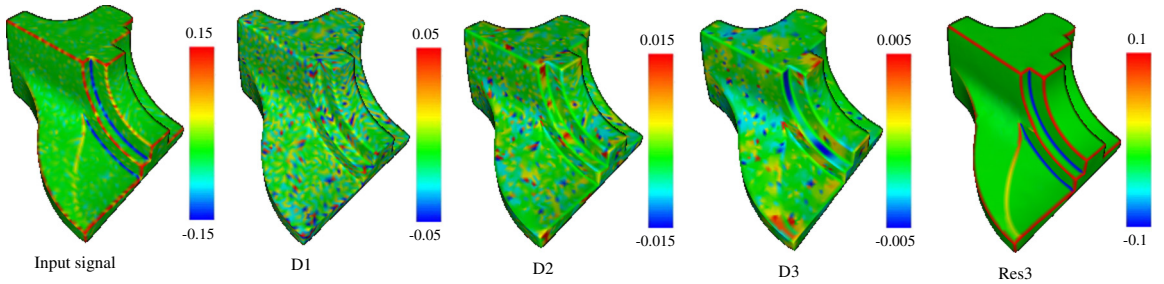

Fig. 5. Feature-preserving multiscale decomposition for the Fandisk model into three levels. The input signal is the measure of mean curvature of the Fandisk model artificially corrupted by Gaussian noise of 5% of mean edge length.

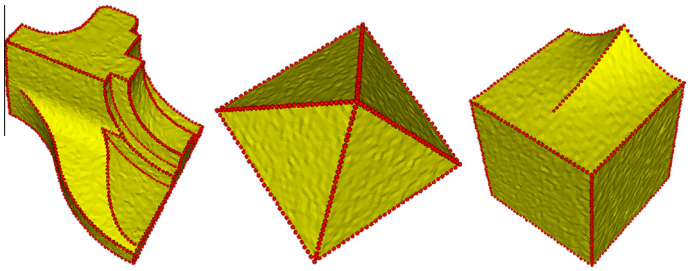

Fig. 6. The feature vertices detected by the method of [37] which are treated as the feature constraints in this paper for the synthetic models corrupted by Gaussian noise of 5% of mean edge length.

$$\|\mathbf{L}\Phi\|^2 + \lambda^2 \sum_{i \in G} |\Phi(\mathbf{v}_i) - \mathbf{g}(\mathbf{v}_i)|^2, \tag{12}$$

with the extremum constraints

$$\Phi(\mathbf{v}_i) = \mathbf{g}(\mathbf{v}_i), \quad i \in C,$$

where λ is the weighting factor for feature vertex positions and its default value is 0.1 in this paper, and $\mathbf{L}$ is the discretized Laplacian matrix with elements computed in Eq. (9) and w_{ij} can be computed for the non-feature vertices using

$$w_{ij} = e^{-|\mathbf{g}(\mathbf{v}_i) - \mathbf{g}(\mathbf{v}_j)|^2 / 2\tau\sigma_s^2}, \quad j \in N(i), \tag{13}$$

and for the feature vertices using

$$w_{ij} = \begin{cases} e^{-|\mathbf{g}(\mathbf{v}_i) - \mathbf{g}(\mathbf{v}_j)|^2 / 2\tau\sigma_s^2}, & j \in N(i) \cap G \\ 0, & \text{otherwise} \end{cases}, \tag{14}$$

where σ_s is the local standard deviation of the original function $\mathbf{g}$ in one ring of the vertex $\mathbf{v}_i$, and τ is a parameter for the user which can control the level of feature enforcement. A smaller parameter means a higher level of feature enforcement, and the default value is 0.6 in this paper, we will discuss it in more details in Section 6.

The energy function (Eq. (12)) can be written as the following form

$$\left\| \begin{bmatrix} \mathbf{L} \\ \lambda \mathbf{F} \end{bmatrix} \Phi - \begin{bmatrix} 0 \\ \lambda \mathbf{g}_G \end{bmatrix} \right\|^2,$$

where $\mathbf{g}_G$ is the original function vector in the feature vertex set G, and $\mathbf{F}$ is a $m \times m$ matrix with elements

$$\mathbf{F}_{ij} = \begin{cases} 1, & j = s_i \in G \\ 0, & \text{otherwise} \end{cases}.$$

This optimization is a linear least-squares optimization problem, which results in the following $(n+m) \times n$ linear system

$$\begin{bmatrix} \mathbf{L} \\ \lambda \mathbf{F} \end{bmatrix} \Phi = \begin{bmatrix} 0 \\ \lambda \mathbf{g}_G \end{bmatrix}, \quad s.t., \ \Phi(\mathbf{v}_i) = \mathbf{g}(\mathbf{v}_i), \quad i \in C, \tag{15}$$

and can be solved by the direct elimination method [5] just like solving the linear system Eq. (8).

5. Surface reconstruction using measure of mean curvature

Once the original surface signal governed by the measure of mean curvature is decomposed into several IMFs or detail levels, we can modify them to generate a new signal $\mathbf{s}'$ about the measure of mean curvature according to the specific needs of surface modeling and processing. We will discuss how to modify them according to the specific applications in Section 6 in more details.

In our framework, a new mesh with vertex positions $\mathbf{V}'$ corresponding to a new signal $\mathbf{s}'$ about the measure of mean curvature can be constructed by a mesh reconstruction method in the least squares sense with the original vertex positions $\mathbf{V}$ as constraints. This idea has been widely used in Laplacian surface processing [26,27]. It is computed by minimizing the following quadratic energy

$$\|\mathbf{L}\mathbf{V}' - \mathbf{s}'\mathbf{N}\|^2 + \mu^2 \sum_{i=1}^{n} \|\mathbf{v}_i' - \mathbf{v}_i\|^2 \tag{16}$$

This energy can be changed into

$$\left\| \begin{bmatrix} \mathbf{L} \\ \mu \mathbf{I}_{n\times n} \end{bmatrix} \mathbf{V}' - \begin{bmatrix} \mathbf{s}'\mathbf{N} \\ \mu \mathbf{V} \end{bmatrix} \right\|^2,$$

and the corresponding $2n \times n$ rectangular linear system $\mathbf{AV}' = \mathbf{b}$ is

$$\begin{bmatrix} \mathbf{L} \\ \mu \mathbf{I}_{n\times n} \end{bmatrix} \mathbf{V}' = \begin{bmatrix} \mathbf{s}'\mathbf{N} \\ \mu \mathbf{V} \end{bmatrix}, \tag{17}$$

where $\mathbf{L}$ is the discretized Laplacian matrix with elements computed using Eq. (9) and w_{ij} is computed using Eq. (2), $\mathbf{N}$ is the vertex normal matrix, μ is the weighting factor for vertex positions and its default value is 0.1 in this paper.

The linear system Eq. (17) can be solved using its normal equation $(\mathbf{A}^T\mathbf{A})\mathbf{V}' = \mathbf{A}^T\mathbf{b}$, which can be efficiently handled by Cholesky factorization.

5.1. Processing open surfaces

During the creation of envelopes in 1D EMD by the interpolation approach, it is difficult to interpolate the data near the two ends because the extrema outside the original signal are unknown. If the two ends are not handled properly, they will give rise to illusive oscillations which will propagate inwards and progressively corrupt the subsequent low frequency IMFs, and this phenomenon is called the end effect [9,10]. These end effects still arise in EMD on open surfaces even though existing EMD methods on 3D surfaces did not explicitly address this deficiency with a proper strategy. For example, the boundary of the residues corresponding to the low frequency IMFs will shrink dramatically when applying the existing algorithm to the coordinates functions of surfaces with boundary (Fig. 7(b)).

Although we could use the measure of mean curvature as the input signal of EMD which would curb such end effect greatly (compared with the method of applying the EMD to the coordinate functions), the shrinkage of boundary is still existing (Fig. 7(c and e)). So we design an alternative method to get rid of this problem. One way is to give more weights on boundary vertices than non-boundary vertices. Specifically, we modify the above-mentioned linear system Eq. (17) during reconstruction as follows:

$$\begin{bmatrix} \mathbf{L}\mathbf{V}' \\ \mu \mathbf{V}'_N \\ \nu \mathbf{V}'_B \end{bmatrix} = \begin{bmatrix} \mathbf{s}'\mathbf{N} \\ \mu \mathbf{V}_N \\ \nu \mathbf{V}_B \end{bmatrix}, \tag{18}$$

where $\mathbf{V}_N$ and $\mathbf{V}_B$ are the original non-boundary vertices and boundary vertices respectively, $\mathbf{V}'_N$ and $\mathbf{V}'_B$ are the new non-boundary vertices and boundary vertices respectively, and ν is the weighting factor for boundary vertices. If ν is set to be much larger than before, the boundary becomes much closer to the original boundary. The default value of ν is 1.0 in this paper. Using this modified scheme, we are able to prevent the boundary shrinkage of the residues (Fig. 7(d)).

6. Experimental results and applications

We have implemented the above framework and tested them on many models including synthetic and scanned meshes. Fig. 3 gives the result about decomposing the measure of mean curvature of the lion model into 3 IMFs using EMD. The meshes corresponding to IMFs are reconstructed by its IMF and the 3rd residue and demonstrate the different scale features of the lion models, i.e., the first IMF represents the finest spatial scale, the second and third IMFs offer much coarser spatial scales. Figs. 4 and 5 give the results about decomposing the signals about the measure of mean curvature of some noisy models with sharp features into three detail levels using our feature-preserving multiscale decomposition method, which treats the noises as details, and the residuals of signals on sharp features can be preserved very well.

In our framework, the different scale features of the 3D surfaces can be extracted by EMD on the measure of mean curvature, thus such framework is highly promising in 3D surface modeling and processing, and many modeling and processing operations can be accommodated, such as filter design, detail transfer, 3D watermark and so on. Furthermore, the features can be preserved by our feature-preserving multiscale decomposition method, we also can conduct some feature-preserving processing applications. In the subsequent sections, we will focus on the applications about filer design, detail transfer, and feature-preserving smoothing and denoising.

6.1. Filter design

Actually, 3D surface filtering can be implemented by enhancing or smoothing IMFs of the measure of mean curvature (i.e., scaling corresponding IMFs), and leaving the residue unchanged:

$$\mathbf{s}' = \sum_{i=1}^{k} \mu(i) \cdot \mathbf{f}_i + \mathbf{r}_k, \tag{19}$$

where $\mathbf{f}_i$ represents the extracted IMFs from the input signal about the measure of mean curvature $\mathbf{s}$, $\mathbf{r}_k$ is the k-th residue, $\mathbf{s}'$ represents the filtering result of $\mathbf{s}$, and $\mu(i)$ are used to control the filtering intensities of different scales. In most cases, the number of IMFs is selected as 3 ($k = 3$ is the default value in this paper), and $\mu(i)$ is selected as linear functions (Fig. 9) which can be used to conduct various 3D surface filtering operations (e.g., low-pass filtering, high-enhancement filtering, band-stop filtering, and band-enhancement filter, etc.) (see Fig. 8).

In addition, all IMFs of the signal about the measure of mean curvature defined on each vertex also carry the spatial information. Thus, we can also interactively process IMFs according to its positional information. Specifically, the user can process IMFs at different parts by different ways, for example, we can use high-enhancement filter to enhance the left foot of Armadillo and use low-pass filter to smooth the right foot of Armadillo (Fig. 10).

Although the surface filtering method using coordinate functions as an input of EMD [34] is related to ours, their method cannot differentiate the features of different scales well since the first IMF almost includes all the detail features and the second IMF and third IMF have few difference (Fig. 8(c and d)). This can also be further demonstrated by the band-enhancement filtering results in

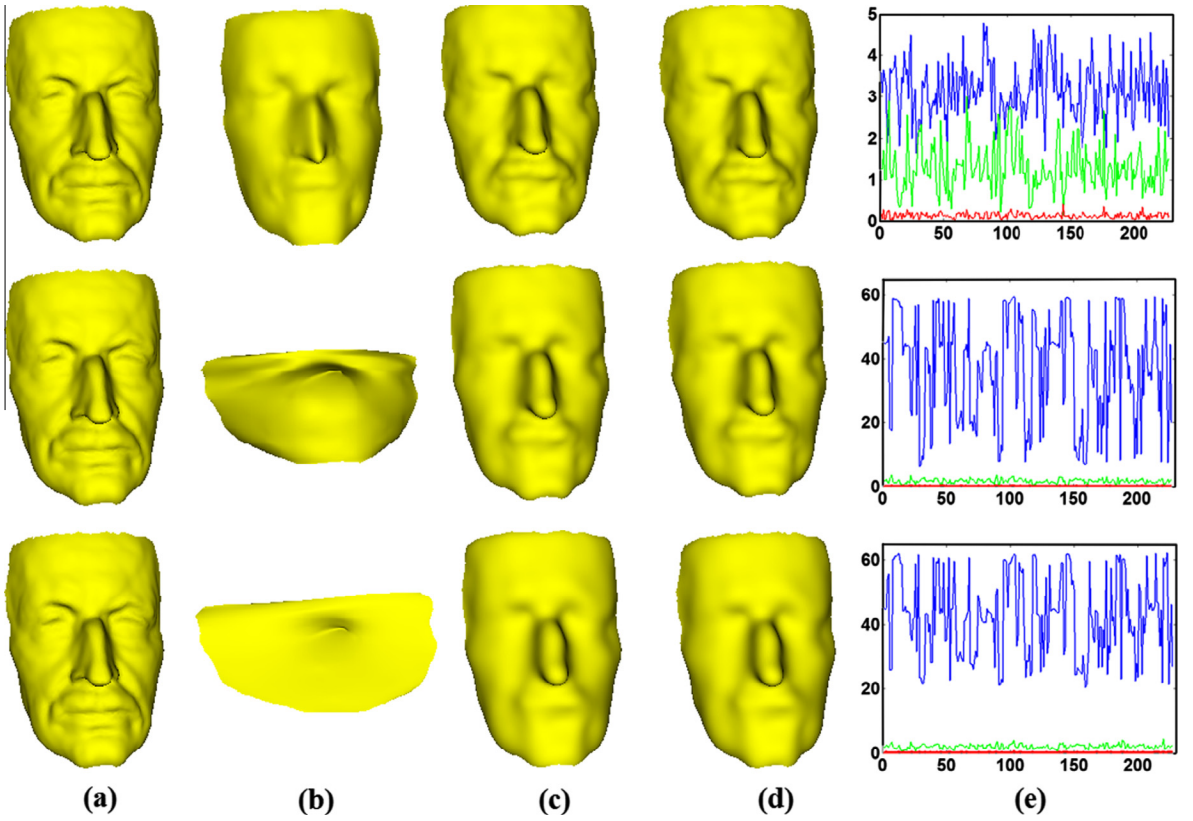

Fig. 7. Result comparison for processing open surfaces. (a) Original model. (b) The method of Wang et al. (c and d) are our methods without and with boundary processing. (e) The error curves between the original boundary and the new boundary with different methods, blue curve, green curve, and red curve corresponds to the results of (b, c, and d), respectively. Meshes of each method from top to bottom correspond to the 1st residue, the 2nd residue and the 3rd residue. (For interpretation of the references to color in this figure legend, the reader is referred to the web version of this article.)

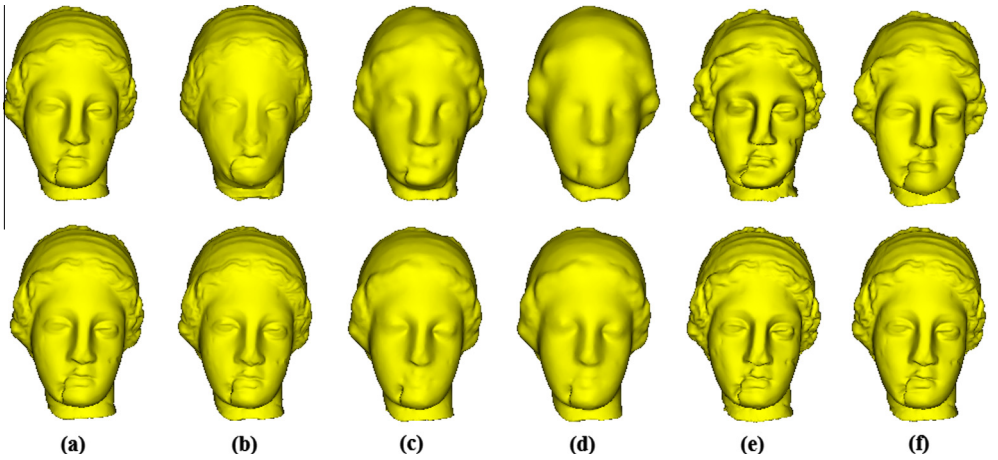

Fig. 8. Various 3D surface filtering comparison for hygeia model between our EMD method (shown in the first row) and the EMD method of Wang et al. (shown in the second row). (a) The original model, (b–f) are the filtering results by using (1,0,0), (0,1,0), (0,0,1), (1,2.5,1) and (1,1,2.5) as the linear filter functions for the corresponding IMFs, respectively.

Fig. 8(e and f). The main reason lies in that 3D surfaces are represented by 3 coordinate functions independent of each other, but the geometry features can only be formulated by collectively making use of all 3 functions. The simple combination of 3 separate decompositions cannot naturally lead to the meaningful computation of any differential features of different scales of the surface. In contrast, the decomposition of our measure of mean curvature can describe the multiscale feature of the original surface perfectly. As for processing open surfaces (Fig. 7), we can see

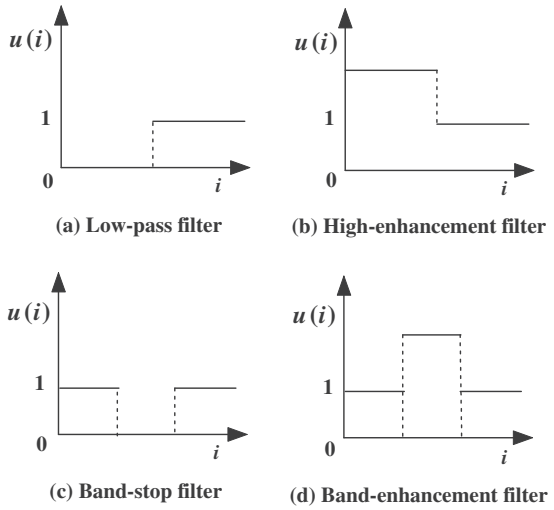

Fig. 9. Linear filter functions.

that the shrinkage of the decomposition on coordinate functions are unacceptable when decomposing the surface after two scales (Fig. 7(b)). The reason lies in that the end effects in EMD are enlarged by decomposing three coordinate functions at the same time. Although the end effect is still existing in our measure of mean curvature for our method (Fig. 7(c)), we can prevent it by adding more constraints at the boundary when reconstructing the surface using the modified IMFs (Fig. 7(d)). Furthermore, their method is pose-dependent as the coordinate functions will have different extrema after changing their poses. Our measure of mean curvature is both rotation and translation invariant, therefore the filtering results using our method are pose-independent.

6.2. Detail transfer

Geometry details are important features of 3D objects. The transfer of details from one shape to another affords a rapid mechanism to create new meaningful models [17,21,28]. In principle, the details are high frequency components of objects, which can be extracted according to several leading IMFs in EMD on the signal about the measure of mean curvature of the model. Therefore, we can conduct detail transfer in our framework effectively.

Before introducing our specific method about detail transfer, let us assume that the source model M_1 and the target model M_2 have the same connectivity and vertices are corresponded to each other beforehand in order that relevant details like facial features of two heads can be transferred into the corresponding positions. If this condition breaks down, we need to select some features as corresponding anchors and parameterize two models onto a common domain, and a remeshing operation can be conducted on both of them in order to generate meshes with the same connectivity [21].

Our detail transfer method first extracts the detail $\mathbf{d}$ of the source model M_1, which can be computed by decomposing its signal about the measure of mean curvature $\mathbf{s}_1$ by EMD,

$$\mathbf{d} = \sum_{i=1}^{k} \mathbf{f}_i, \tag{20}$$

where $\mathbf{f}_i,\ i = 1, \ldots, k$ are the leading IMFs from the measure of mean curvature $\mathbf{s}_1$, and k is the decomposition level which can be selected by a user and represents the range of detail that the user wishes to transfer (The default value is set to be 3 in our paper). Then the signal about the measure of mean curvature $\mathbf{s}_2$ of the target model can be modified by adding the detail $\mathbf{d}$ of the source model

$$\mathbf{s}_2' = \mathbf{s}_2 + \mathbf{d}. \tag{21}$$

Finally, the detail transfer model can be reconstructed by the new signal about the measure of mean curvature $\mathbf{s}_2'$ according to the reconstruction system of the target surface M_2.

Fig. 11 shows the results about transferring the detail of Hygeia to Manniquin and Cat-head, we can see that the two new models not only have the detail of Hygeia but also preserve the global shape of the original models.

6.3. Feature-preserving smoothing and denoising

For the task of feature-preserving smoothing and denoising, we have used our feature-preserving multiscale method to decompose the signal about the measure of mean curvature and treated the surface reconstructed

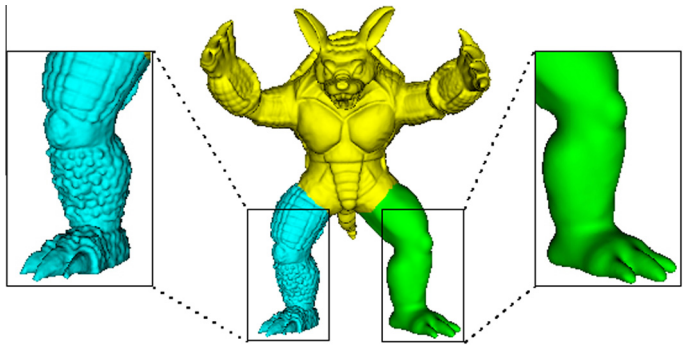

Fig. 10. Local filtering on Armadillo model. The left foot is processed by high-enhancement filter while the right foot is smoothed by low-pass filter.

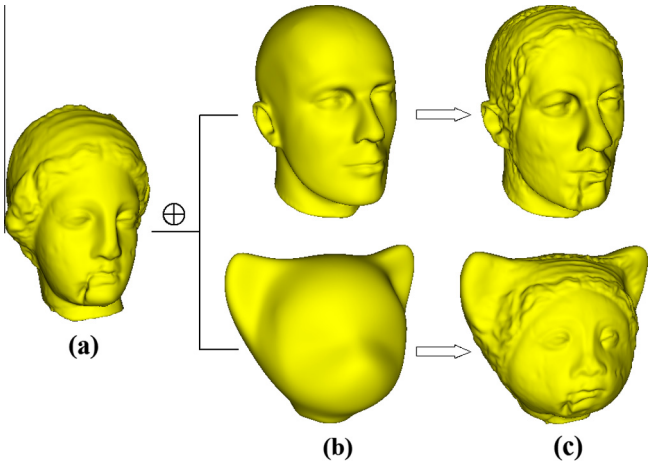

Fig. 11. Detail transfer results (c) from Hygeia (a) to Manniquin (top) and Cat-head (bottom) in (b).

using the residue as the smoothing result. Sharp features such as sharp edge and corners of synthetic models are extracted by the existing method [37] during the pre-processing stage. In addition, we need to update the normals before updating the vertex positions in order to better reconstruct the smoothing surface by using

$$\mathbf{n}_i' = \frac{1}{\sum_{j\in N(i)}} \sum_{j\in N(i)} \mathbf{s}(\mathbf{v}_i)\mathbf{n}_i. \tag{22}$$

We shall demonstrate the results about feature-preserving surface smoothing on synthetic meshes with sharp edges and corners, which are also perturbed by some Gaussian noise (Figs. 4, 12 and 13). We also show some results about feature-preserving surface smoothing on surfaces scanned from real world physical prototypes which exhibit both noises and holes (Fig. 14). We can see that our method can remove noises of the models and preserve the features such as the sharp edges and corners.

As documented before our method is an extension of the edge-preserving multiscale image decomposition based on extremal envelopes, the feature-preserving smoothing on surfaces is more complicated than that of 2D images as the sharp edges and corners will be smoothed when extracting details by subtracting the average of extremal envelopes interpolated from local extrema (Fig. 4). By explicitly tagging the sharp feature vertices as constraints extracted prior to multiscale decomposition, we cannot only remove the noise of the models but also preserve the sharp features.

We compare our method with the global Laplacian smoothing method which also makes use of the explicit features as constraints [13,18]. In Fig. 12, we can see that those methods cannot preserve the sharp features when only vertex constraints are enforced. More constraints such as face barycenter constraints, and coplanar constraints must be added in order to better preserve features in those methods. In addition, it is extremely hard to control if we add other types of constraints. Therefore we choose not to investigate whether our method can outperform their methods when more constraints are added into the surface reconstruction processing. In addition, our method can generate good results without the explicit feature constraints if models have no sharp edges and corners while their methods always need these feature constraints (Fig. 14).

We compare our method with the bilateral filtering method [4]. As explicitly documented in the introduction of [29], the bilateral filtering technique is effective in smoothing variation with small amplitude, it necessarily blurs sharp edges that have smaller magnitudes of gradients more than the oscillations to be smoothed. Therefore

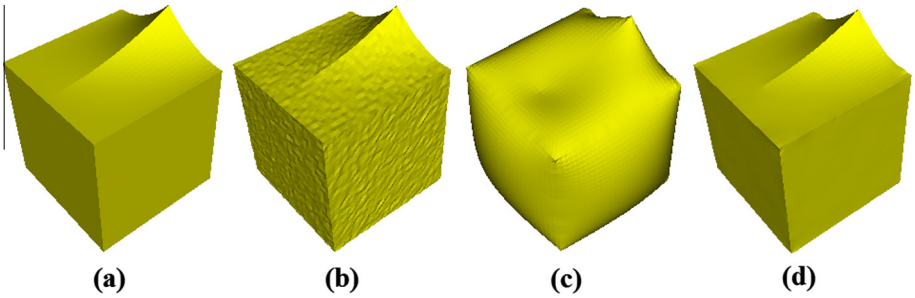

Fig. 12. Comparison with global Laplacian smoothing with feature constraints. (a) The original cubic model as a ground truth. (b) The cubic model artificially corrupted by 5% Gaussian noise of mean edge length. (c) Global Laplacian smoothing with feature constraints with 10 as weight. (d) The mesh corresponding to the 3th residue using by our feature-preserving multiscale decomposition.

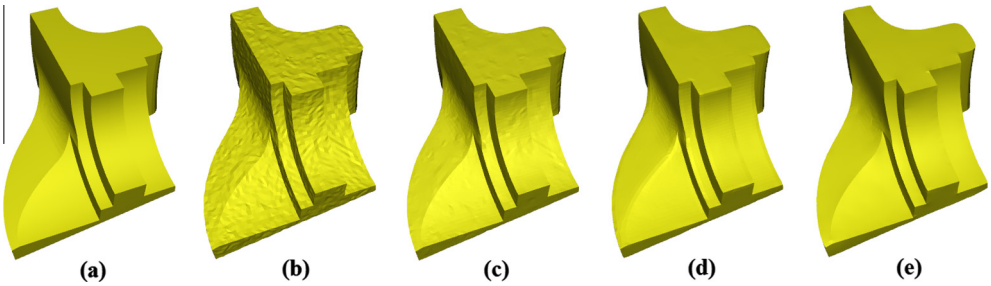

Fig. 13. Comparison with bilateral filtering. (a) The Fandisk model as a ground truth. (b) The model artificially corrupted by 5% Gaussian noise of mean edge length. (c) Perform a smoothing operation 3 times by bilateral filtering with the parameter $\sigma_c = 0.4\rho$, and $\sigma_s = 0.025\rho$, ρ is the mean edge length of the mesh. (d) Perform a smoothing operation 3 times by bilateral filtering with much larger parameter $\sigma_c = 0.4\rho$, and $\sigma_s = 0.05\rho$. (e) The mesh reconstructed using 3rd residue of our method.

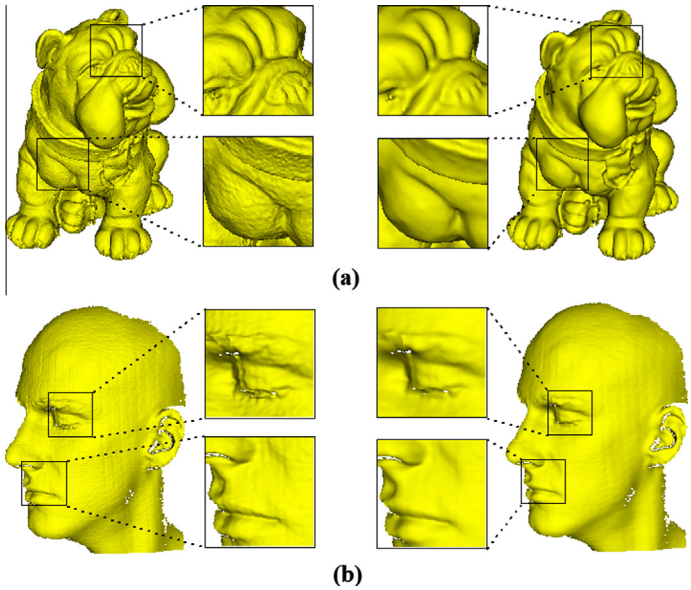

Fig. 14. Smooth the models (left) with real world noise. The results (right) are generated by reconstructing the 3rd residue of our feature-preserving multiscale decomposition method.

it is difficult to choose the best intervals of spatial locations for signals. In contrast, our smoothing algorithm smoothes large oscillations and strictly preserves sharp edges, without the need of careful selection of parameter values (Fig. 13).

It may be noted that, Wang et al. [34] also proposed an approach based on extremal envelopes to conduct multiscale surface decomposition with the feature-preserving property, which made an attempt to extend the edge-preserving multiscale image decomposition method [29] to 3D surfaces. Nevertheless, by examining the experiment on Fandisk model in Fig. 12 of [34] and making a comparison with Fig. 13(e), it is apparent that our method outperforms their method. In addition, their method cannot process open surfaces while our method can support this functionality with much better results.

6.4. Time performance and parameters

We implement our method in matlab 2012 on a laptop with Inter Core (TM) i5-3230 CPU @ 2.60 GHz, 2.60 GHz, and with 8.0 GB RAM. The main time-consuming part of our method is the decomposition of the signal about the measure of mean curvature. EMD requires an iterate sifting process to extract each IMF and two linear systems are solved in each iteration. Our feature-preserving multiscale decomposition uses only one feature-preserving smoothing step to extract each detail level instead of the iterate sifting process in order to accelerate the decomposition. Another time consuming part is the surface reconstruction step which needs to solve a sparse linear system. In all our experiments the signals about the measure of mean curvature are decomposed into three levels which is usually enough in many geometric modeling and processing tasks. Hence, our method is fast and efficient. All the timing statistics of tested models are documented in Table 1.

Two parameters in our method need to be further discussed. One is the extremum detection parameter t in feature-preserving multiscale decomposition, which should be set to be much smaller in order to extract more extremum for the objects with rich features (0.6 is used to obtain results shown in Fig. 14). The other is the feature-preserving

Table 1
Run time and parameter statistics. EMD: time of using EMD. FPMD: time of using the feature-preserving multiscale decomposition. SR: surface reconstruction time using the new signal about the measure of mean curvature. Total: total time.

Figures	#Vertices	Parameters					Timing (s)			
		t	λ	τ	μ	ν	EMD	FPMD	SR	Total
3	30,563				0.1		4.26		0.29	5.08
4	4098	0.8	0.1	0.3	0.1			0.34	0.04	0.51
5&13	6475	0.8	0.1	0.3	0.1			0.56	0.08	0.93
7	4486				0.1	1.0	0.5		0.05	0.67
8	13,460				0.1		1.53		0.13	1.95
10	172,974				0.1		26.88		2.21	32.06
12	6177	0.8	0.1	0.3	0.1			0.55	0.07	0.98
14(a)	501,500	0.6		0.6	0.1			36.82	10.41	53.35
14(b)	60,754	0.6		0.6	0.1	1.0		3.93	0.55	5.65

parameter τ for the extremum envelope computation, which should be set much smaller in order to preserve the sharp features (0.3 is used to generate results shown in Figs. 4, 12 and 13). All other parameters can be set to be default values while guaranteeing satisfactory results, such as the constraint parameters μ and ν for non-boundary and boundary vertex positions for surface reconstruction respectively, and the feature constraint parameter λ of the extrema envelope computation for the feature-preserving multiscale decomposition. All parameters used in our experiments are also documented in Table 1.

6.5. Limitation

Our feature-preserving multiscale decomposition method must detect sharp features of 3D surfaces in a preprocessing stage. Unfortunately, if the models are corrupted by large amount of noise it is much more challenging to detect sharp features. If sharp features cannot be identified properly, processed models will be blurred when we try to smooth the models. To ameliorate, we believe that it is more promising to implicitly define features in our feature-preserving multiscale decomposition algorithm, for example, one promising approach is to incorporate more powerful sparse modeling tools into our surface processing framework. This will be our future work next.

7. Conclusion

With a goal of realizing the full potential of EMD for 3D surface modeling and processing in mind, we have developed a framework based on the improved, feature-centric EMD formulation in this paper. Our system first employs a measure of mean curvature as an input of EMD, and then conduct its EMD operation to acquire several IMFs (that encode features at different scales), which can enable 3D surface modeling and processing to be both powerful and efficient by only editing the IMFs. More importantly, the theoretical originality of this paper results from a novel feature-sensitive multiscale decomposition algorithm enabled by our feature-preserving EMD formulation. The core idea is to explicitly formulate details as oscillation between local minima and maxima.

Within our novel framework, potential applications are widespread, and we can accommodate many modeling and processing operations, such as filter design, detail transfer, and feature-preserving smoothing and denoising. Experiments and comparisons on popularly-used geometric models have effectively demonstrated that our surface processing method based on EMD and our feature-preserving multiscale decomposition can guarantee excellent results and has shown greater promise to broaden their application scopes towards more powerful digital geometry modeling and processing.

Acknowledgments

We thank all the anonymous reviewers for their valuable comments. This work is supported in part by National Science Foundation of USA (IIS-0949467, IIS-1047715, and IIS-1049448), National Natural Science Foundation of China (Nos. 61190120, 61190121, 61190125, 61202261, 61173102, 61173103), China Scholarship Council, Scientific and Technological Development Plan of Jilin Province (No. 20130522113JH), and open fund from Key Laboratory of Symbolic Computation and Knowledge Engineering of Ministry of Education of China (No. 93K172012K02). Models are courtesy of AIM@SHAPE Repository.

References

[1] C.L. Bajaj, G. Xu, Anisotropic diffusion of surfaces and functions on surfaces, ACM Trans. Graph. 22 (1) (2003) 4–32.
[2] U. Clarenz, U. Diewald, M. Rumpf, Anisotropic geometric diffusion in surface processing, in: IEEE Visualization, 2000, pp. 397–405.
[3] R.R. Coifman, M. Maggioni, Diffusion wavelets, Appl. Comput. Harmon. Anal. 21 (1) (2006) 53–94.
[4] S. Fleishman, I. Drori, D. Cohen-Or, Bilateral mesh denoising, ACM Trans. Graph. 22 (3) (2003) 950–953.
[5] M.S. Floater, K. Hormann, Parameterization of triangulations and unorganized points, in: A. Iske, E. Quak, M.S. Floater (Eds.), Tutorials on Multiresolution in Geometric Modelling, Springer, Berlin, Heidelberg, 2002, pp. 287–316, (Mathematics and Visualization).
[6] I. Guskov, W. Sweldens, P. Schröder, Multiresolution signal processing for meshes, in: SIGGRAPH, 1999, pp. 325–334.
[7] T. Hou, H. Qin, Admissible diffusion wavelets and their applications in space–frequency processing, IEEE Trans. Vis. Comput. Graph. 19 (1) (2013) 3–15.
[8] H. Huang, J. Pan, Speech pitch determination based on Hilbert–Huang transform, Signal Process. 86 (4) (2006) 792–803.
[9] N.E. Huang, Z. Shen, S.R. Long, M.C. Wu, H.H. Shih, Q. Zheng, N.C. Yen, C.C. Tung, H.H. Liu, The empirical mode decomposition and the hilbert spectrum for nonlinear and non-stationary time series

analysis, Proc. Roy. Soc. Lond. Ser. A: Math., Phys. Eng. Sci. 454 (1971) (1998) 903–995.
[10] N.E. Huang, Z. Wu, A review on Hilbert–Huang transform: method and its applications to geophysical studies, Rev. Geophys. 46 (2) (2008) 1–23.
[11] A. Levin, D. Lischinski, Y. Weiss, Colorization using optimization, ACM Trans. Graph. 23 (3) (2004) 689–694.
[12] A. Linderhed, 2-d empirical mode decompositions in the spirit of image compression, in: Wavelet and Independent Component Analysis Applications IX, 2002, pp. 1–8.
[13] L. Liu, C.L. Tai, Z. Ji, G. Wang, Non-iterative approach for global mesh optimization, Comput.-Aided Des. 39 (9) (2007) 772–782.
[14] M. Lounsbery, T.D. DeRose, J. Warren, Multiresolution analysis for surfaces of arbitrary topological type, ACM Trans. Graph. 16 (1) (1997) 34–73.
[15] D.P. Mandic, N. ur Rehman, Z. Wu, N.E. Huang, Empirical mode decomposition-based time–frequency analysis of multivariate signals: the power of adaptive data analysis, IEEE Signal Process. Mag. 30 (6) (2013) 74–86.
[16] M. Meyer, M. Desbrun, P. Schröder, A.H. Barr, Discrete differential-geometry operators for triangulated 2-manifolds, in: H.C. Hege, K. Polthier (Eds.), Visualization and Mathematics III, Springer, 2002, pp. 113–134 (Mathematics and Visualization).
[17] M. Mousa, R. Chaine, S. Akkouche, E. Galin, Efficient spherical harmonics representation of 3d objects, in: M. Alexa, S.J. Gortler, T. Ju (Eds.), Pacific Conference on Computer Graphics and Applications, IEEE Computer Society, 2007, pp. 248–255.
[18] A. Nealen, T. Igarashi, O. Sorkine, M. Alexa, Laplacian mesh optimization, in: Y.T. Lee, S.M.H. Shamsuddin, D. Gutierrez, N.M. Suaib (Eds.), GRAPHITE, ACM, 2006, pp. 381–389.
[19] O. Niang, A. Thioune, M.C.E. Gueirea, r. Delchelle, J. Lemoine, Partial differential equation-based approach for empirical mode decomposition: application on image analysis, IEEE Trans. Image Process. 21 (9) (2012) 3991–4001.
[20] M. Pauly, M.H. Gross, Spectral processing of point-sampled geometry, in: SIGGRAPH, 2001, pp. 379–386.
[21] E. Praun, W. Sweldens, P. Schröder, Consistent mesh parameterizations, in: SIGGRAPH, 2001, pp. 179–184.
[22] X. Qin, X. Chen, S. Zhang, W. Wang, EMD based fairing algorithm for mesh surface, in: 11th IEEE International Conference on Computer Aided Design and Computer Graphics, IEEE, 2009, pp. 606–609.
[23] N. Rehman, D.P. Mandic, Empirical mode decomposition for trivariate signals, IEEE Trans. Signal Process. 58 (3) (2010) 1059–1068.
[24] T.M. Rutkowski, D.P. Mandic, A. Cichocki, A.W. Przybyszewski, EMD approach to multichannel eeg data – the amplitude and phase components clustering analysis, J. Circ., Syst., Comput. 19 (1) (2010) 215–229.
[25] P. Schröder, W. Sweldens, Spherical wavelets: efficiently representing functions on the sphere, in: Proceedings of the 22nd Annual Conference on Computer Graphics and Interactive Techniques, in: SIGGRAPH '95, 1995, pp. 161–172.
[26] O. Sorkine, Differential representations for mesh processing, Comput. Graph. Forum 25 (4) (2006) 789–807.
[27] O. Sorkine, D. Cohen-Or, Least-Squares Meshes, in: SMI, IEEE Computer Society, 2004, pp. 191–199.
[28] O. Sorkine, D. Cohen-Or, Y. Lipman, M. Alexa, C. Rössl, H.P. Seidel, Laplacian surface editing, in: Proceedings of the 2004 Eurographics/ACM SIGGRAPH Symposium on Geometry Processing, 2004, pp. 175–184.
[29] K. Subr, C. Soler, F. Durand, Edge-preserving multiscale image decomposition based on local extrema, ACM Trans. Graph. 28 (5) (2009) 1–9.
[30] G. Taubin, A signal processing approach to fair surface design, in: SIGGRAPH, 1995, pp. 351–358.
[31] G. Taubin, Linear anisotropic mesh filtering, in: IBM Research Report RC22213, 2001.
[32] B. Vallet, B. Levy, Spectral geometry processing with manifold harmonics, Comput. Graph. Forum 27 (2) (2008) 251–260.
[33] H. Wang, H. Chen, Z. Su, J. Cao, F. Liu, X. Shi, Versatile surface detail editing via Laplacian coordinates, Vis. Comput. 27 (5) (2011) 401–411.
[34] H. Wang, Z. Su, J. Cao, Y. Wang, H. Zhang, Empirical mode decomposition on surfaces, Graph. Models 74 (4) (2012) 173–183.
[35] J. Wang, X. Zhang, Z. Yu, A cascaded approach for feature-preserving surface mesh denoising, Comput.-Aided Des. 44 (7) (2012) 597–610.
[36] S. Wang, T. Hou, Z. Su, H. Qin, Multi-scale anisotropic heat diffusion based on normal-driven shape representation, Vis. Comput. 27 (6–8) (2011) 429–439.
[37] X. Wang, J. Cao, X. Liu, B. Li, X. Shi, Y. Sun, Feature detection of triangular meshes via neighbor supporting, J. Zhejiang Univ. – Sci. C 13 (6) (2012) 440–451.
[38] M.H. Yeh, The complex bidimensional empirical mode decomposition, Signal Process. 92 (2) (2012) 523–541.
[39] S. Yoshizawa, A. Belyaev, H.P. Seidel, Smoothing by Example: Mesh Denoising by Averaging with Similarity-based Weights, in: SMI, IEEE Computer Society, Washington, DC, USA, 2006, pp. 38–44.
[40] Y. Zheng, H. Fu, O.K.C. Au, C.L. Tai, Bilateral normal filtering for mesh denoising, IEEE Trans. Vis. Comput. Graph. 17 (10) (2011) 1521–1530.
[41] K. Zhou, H. Bao, J. Shi, 3d surface filtering using spherical harmonics, Comput.-Aided Des. 36 (4) (2004) 363–375.